Adsorption (2014) 20:37–52
DOI 10.1007/s10450-013-9547-y

Standing wave design of a four-zone thermal SMB fractionator and concentrator (4-zone TSMB-FC) for linear systems

Nicholas Soepriatna · N. H. Linda Wang · Phillip C. Wankat

Received: 10 January 2013 / Accepted: 25 April 2013 / Published online: 8 May 2013

Abstract For a dilute feed, a four-zone SMB with temperature gradient (4-zone TSMB-FC) can fractionate and simultaneously concentrate two solutes. Optimization of the operating parameters for this system, which include four zone flow rates and port switching time, is a major challenge because of the five variables. Initial choice of the variables using the triangle theory followed by a systematic search using rate model simulations is time-consuming. In this study, the SWD developed previously for isothermal systems is modified for the first time for a 4-zone TSMB-FC. The optimum operating parameters are determined with the new method. Only linear isotherm systems with significant mass transfer resistances are considered. For a dilute feed, a 4-zone SMB-FC can produce pure desorbent, in addition to extract and raffinate products with high purities. For the separation of *p*-xylene and toluene with silica gel in the temperature range from 0 to 80 °C, the enrichment factor in the linear region can be as high as 80 fold for an extract purity of 99.99 % and tenfold for raffinate purity of 99.8 %, while withdrawing the desorbent at a desorbent to feed flow rate ratio of 0.53 and 0.78, respectively.

Keywords Concentration · Standing wave design · Simulated moving bed · Adsorption · Thermal swing adsorption

List of symbols

A_i	Pre-exponential factor of the Arrhenius equation (L g^{-1})
c	Concentration of solute in the liquid phase (g L^{-1})
c_i^*	Concentration of solute i in the pore phase (g L^{-1})
$c_{D,\ i}$	Concentration of solute i in the desorbent stream (g L^{-1})
$c_{F,\ i}$	Concentration of solute i in the feed (g L^{-1})
$c_{Fb,\ i}$	Concentration of solute i before the feed port (g L^{-1})
$c_{FP,\ i}$	Concentration of solute i after the feed port (g L^{-1})
$c_{R,\ i}$	Concentration of solute i in the raffinate stream (g L^{-1})
$c_{E,\ i}$	Concentration of solute i in the extract stream (g L^{-1})
C_{pL}	Heat capacity of the liquid phase (J g^{-1} K^{-1})
C_{pS}	Heat capacity of the solid phase (J g^{-1} K^{-1})
D	Desorbent flow rate (mL min^{-1})
$D_{ax,i,j}$	Axial dispersion coefficient of solute i in zone j (cm^2 min^{-1})
$D_{ax,E}$	Thermal axial dispersion coefficient (cm^2 min^{-1})
EF	Enrichment factor
K_{di}	Size exclusion factor
$k_{f,i,j}$	Mass transfer coefficient of solute i in zone j (LDF) (min^{-1})
$k_{f,i}a_p$	Effective mass transfer coefficient (min^{-1})
$K(T)$	Temperature dependent equilibrium constant (L g^{-1})
L	Column length (cm)
P	Bed phase ratio
PI	Purity index (average purity of the raffinate and extract stream)
$P_{R,\ i}$	Purity of solute i in the raffinate stream (%)
$P_{E,\ i}$	Purity of solute i in the extract stream (%)
q	Concentration of solute in the solid phase (g L^{-1})
$\overline{q}$	Average concentration of solute in the solid phase (g L^{-1})
F	Volumetric flow rate of the feed (mL min^{-1})

N. Soepriatna · N. H. L. Wang · P. C. Wankat (✉)
School of Chemical Engineering, Purdue University,
480 Stadium Mall Dr., West Lafayette, IN 47906, USA
e-mail: wankat@purdue.edu

Q_j Volumetric flow rate of zone j (mL min^{-1})
R Ideal gas constant (J K^{-1} mol^{-1})
S Column cross-sectional area (cm^2)
T Temperature (K)
$u_{i,j}$ Solute wave velocity of solute i in zone j (cm min^{-1})
u_{port} Port velocity (cm min^{-1})
$\bar{u}_{o,j}$ Interstitial velocity of the mobile phase in zone j (cm min^{-1})
$u_{o,j}$ Zone linear velocity in zone j (cm min^{-1})
Y_i Yield of solute i
ΔH Heat of adsorption (J mol^{-1})
β_j^i Decay coefficient of solute i in zone j
$\delta_{i,j}$ Retention factor of solute i in zone j
ε_e Bed void fraction
ε_p Intra-particle void fraction
ρ_L Density of the liquid phase (g mL^{-1})
ρ_S Density of the solid phase (g mL^{-1})

1 Introduction

1.1 Background

Simulated moving bed (SMB) is an efficient separation process because it mimics a true moving bed (TMB). Several fixed beds are connected to form a loop, with counter-current movement of the two phases simulated by intermittent switching of inlet (feed and desorbent) and outlet (raffinate and extract) ports. High loading of a binary mixture can be achieved in the loop with two large overlapping solute bands. Feed is introduced in the region where the two bands overlap, while two pure products are drawn separately from the regions where the bands do not overlap. High adsorbent utilization, low desorbent usage, and continuous separation can be obtained in such a configuration.

SMB systems have been extensively used in the petrochemical industry since its first successful commercialization by UOP for hydrocarbon separations in the 1960's. It was initially used in the Molex process to separate paraffins from branched-chain and cyclic isomers (Broughton and Carson 1959). UOP's largest SMB success is the Parex process that produces high purity *p*-xylene from C_8 aromatics (Broughton et al. 1970). Eventually, SMB gained popularity in the separations industry because of the benefits of high productivity, high product purity, and low desorbent consumption. This technology is currently used in various large-scale industrial processes for the separations of sugars (Azevedo and Rodrigues 2001; Beste et al. 2000), fine chemicals, and pharmaceutical products (Negawa and Shoji 1992; Francotte and Richert 1997; Guest 1997; Pais et al. 1998). Aside from fractionation, SMB type systems also show potential for process intensification of other unit operations (Murthy et al. 2008; Sivakumar and Rao 2012).

The most common SMB system used in industries is an isothermal four-zone SMB system (Wankat 2012). Various configurations and strategies to improve the four-zone SMB performance have been reported in the literature. Examples include one-zone SMB analogs (Abunasser et al. 2003; Abunasser and Wankat 2006), two-zone SMBs (Lee 2000; Jin and Wankat 2005), three-zone SMBs (Zang and Wankat 2002), five-zone SMBs (Kim et al. 2004; Xie et al. 2005), nine-zone SMBs (Wooley et al. 1998; Nicolaos et al. 2001), Power Feed operation (Zhang et al. 2003), Partial Feed operation (Zang and Wankat 2002), ModiCon (Schramm et al. 2003), VariCol (Ludemann-Hombourger et al. 2000), enriched-extract SMB (Paredes et al. 2006), feedback SMB (Keβler and Seidel-Morgenstern 2008), and tandem SMB systems (Hritzko et al. 2002; Xie et al. 2002). Despite all the aforementioned strategies, there is still more room for reducing solvent consumption, increasing productivity, and increasing product purity.

Operation of an SMB with temperature, solvent strength, and/or pH gradient can improve all three performance factors. Gradient operation is advantageous compared to other strategies because each zone can be operated under conditions optimal to its respective role (adsorption, desorption, or separation of solutes). The temperature gradient operated SMB fractionation systems (TSMB) have been rigorously studied by Ching and Ruthven (1986), Migliorini et al. (2001), Kim et al. (2005), Jin and Wankat (2007), and others. Compared to the use of other gradients, thermal gradients have the advantage of not requiring additional chemicals; however, thermal gradient performance can be limited by thermal degradation and systems that have little temperature dependence of the isotherms (e.g., fructose and glucose separation on ion exchange resin in calcium form). The major advantage of the TSMB is the significant reduction in solvent consumption used for column regeneration that results in major energy savings in solvent recovery. These studies showed that the travelling wave heating mode is preferred because it can be scaled up. Furthermore, the temperature gradient allows TSMB to work as a concentrator (Lee and Wankat 2011).

1.2 Motivation/importance

The local equilibrium theory or the triangle theory is widely used for designing SMB systems. This method is simple and the solute movement within the columns can be easily visualized (Storti et al. 1993; Mazzotti et al. 1997; Migliorini et al. 1998). However, the local equilibrium

theory only applies to an ideal system, which does not have any mass transfer or dispersion effects. In reality, mass transfer effects are significant for low pressure systems (or non-ideal systems). After the local equilibrium theory is used to identify an acceptable region, a large number of rate model simulations are still required to determine the optimal design for a non-ideal system. Here the optimal is defined as the operating zone flow rates and port switching time which gives the lowest solvent consumption for a given SMB zone configuration. Recognizing the need for a more efficient design method, Ma and Wang (1997) developed a powerful design method called the standing wave design (SWD). This method applies to non-ideal systems because it takes into account mass transfer and axial dispersion effects, and enables direct calculation of the optimal designs for isothermal systems as shown in Fig. 1.

1.3 Objective/scope

The purpose of this study is to extend the linear SWD method for isothermal 4-zone SMB systems to a 4-zone TSMB system to find the optimal design for fractionation and concentration. This system will be referred to as the 4-zone thermal SMB fractionator and concentrator (4-zone TSMB-FC). The complete cycle schematic is shown in Fig. 2, where *A* is the raffinate product (low affinity solute) and *B* is the extract product (high affinity solute). The key parameters affecting the purity of the products as well as its enrichment factor (EF) will be investigated along with the concentration and temperature dynamics within the columns.

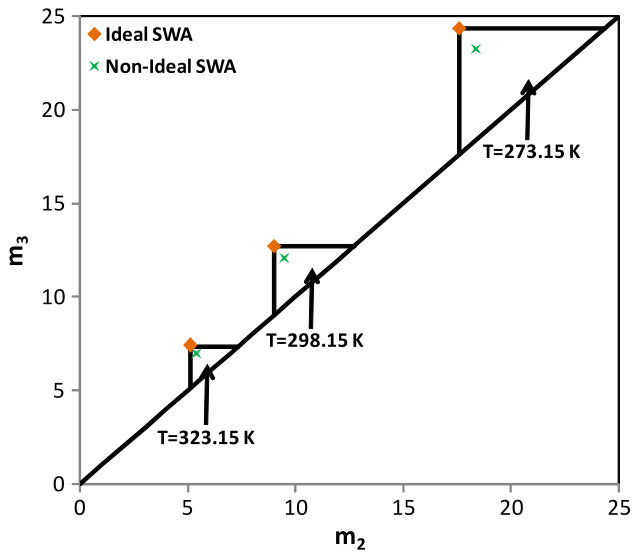

Fig. 1 Standing wave design results in the triangular region of the triangle theory for isothermal 4-zone SMB system at different temperatures. (The vertex is the optimum operating condition for a local equilibrium system)

1.4 Method/approach

The SWD method is extended to non-isothermal operation to determine the optimal 4-zone TSMB-FC design for the separation of dilute mixtures. The optimal design for a given temperature gradient, feed flow rate, and zone configuration, is defined as the operating conditions that give the lowest desorbent usage (or D/F) for the specified yields for both solutes. The lowest D/F also means the highest EFs for the extract and the raffinate.

The SWD concept is developed by solving the steady state analytical solutions for linear isotherms for the zone velocities (and thus the flow rates of each zone and the switching time or port velocity). Since the detailed derivation for isothermal systems can be found in Ma and Wang (1997), only a brief explanation of the SWD derivation is given here (refer to Appendix 1 for detailed derivation). For a given temperature gradient and zone configuration, the operating conditions are first determined using the SWD method. To explore the effects of temperature change, Aspen Chromatography simulations are used to obtain the purities, EFs, and D/F and to plot the concentration and temperature profiles. The performance of the designs for various temperature gradients and zone configurations are compared. The results show that for a dilute feed, it is possible to obtain high purity products and withdraw pure desorbent (D/F < 0) using a 4-zone TSMB-FC.

1.5 Novelty and significance

There are three main differences between the 4-zone TSMB-FC discussed in this study and previous studies on conventional SMB systems and thermal SMB concentrator systems. First, the TSMB-FC system simultaneously fractionates and concentrates the two solutes. An isothermal 4-zone SMB only fractionates the two solutes. A thermal SMB concentrator only concentrates a single solute. Thus, the 4-zone TSMB-FC system combines the role of a 4-zone isothermal SMB with that of a thermal SMB concentrator. Second, the SWD method was extended to a non-isothermal 4-zone TSMB-FC. The results of this study show that this design method determines the optimal design directly without extensive simulation trials. Third, it is shown for the first time that a 4-zone TSMB-FC based on the SWD can produce two high purity products plus pure desorbent. The Aspen simulations show that the product purity, yield, and D/F of the simulated processes are in close agreement with the target values used in the SWD and desorbent indeed can be withdrawn.

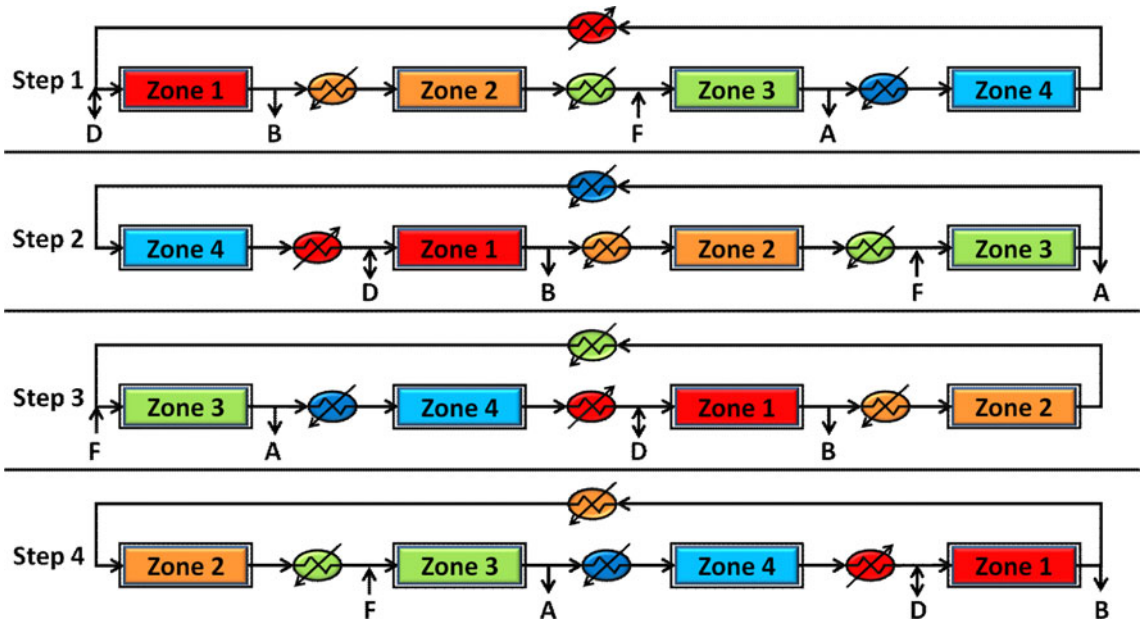

Fig. 2 4-zone TSMB-FC schematic operation with one column per zone

2 Theory

2.1 4-zone TSMB operation and basic equations

A 4-zone TSMB-FC system operates with decreasing temperatures ($T_1 > T_2 > T_3 > T_4$) as shown in Fig. 2. Zones 1 and 2 are at higher temperatures to facilitate desorption of a high affinity solute (B) and a low affinity solute (A), respectively. Zones 3 and 4 are operated at lower temperatures to facilitate adsorption. Zone 1 is the column regeneration zone, where the strongly adsorbed solute B is displaced by the high temperature desorbent. Separation of the two solutes occurs in zones 2 and 3 since solute A has a higher migration velocity than solute B. The port velocity is between the two solute migration velocities, resulting in a net shift of the solute A band towards the raffinate port and solute B band towards the extract port. Operating zones 2 and 3 at different temperatures increases the differences in the solute velocities. Zone 4 acts as the desorbent purification zone, where the weakly adsorbed solute A adsorbs. To make sure that the roles of all four zones are satisfied, the following inequalities must be satisfied:

$$u_{A,2},\ u_{A,3} > u_{port} > u_{A,4} \tag{1a}$$

$$u_{B,1} > u_{port} > u_{B,2},\ u_{B,3} \tag{1b}$$

where u_{port} is the port velocity and $u_{i,j}$ is the migration velocity of solute i in zone j.

The system considered is the separation of p-xylene and toluene using silica gel as the adsorbent and n-heptane as the solvent (desorbent), which does not adsorb. The system parameters in the mass and energy balances and used in the detailed simulations are listed in Table 1. The adsorption isotherms for p-xylene and toluene in this study are (Matz and Knaebel 1991);

$$q = K(T)c; \quad K(T) = A_i \exp\left(-\frac{\Delta H}{RT_j}\right) \tag{2a, b}$$

$$p\text{-xylene: } q_{px} = 0.0105 \exp\left(\frac{2115.1}{T}\right) c_{px} \tag{2c}$$

$$\text{toluene: } q_{tol} = 0.0061 \exp\left(\frac{2175.3}{T}\right) c_{tol} \tag{2d}$$

where $K(T)$ is temperature dependent equilibrium constant, c is the solute concentration in the mobile phase, q is the solute concentration in the stationary phase, and A_i, ΔH, R, and T_j are the pre-exponential factor, heat of adsorption, ideal gas constant, and the temperature of the system at zone j, respectively. Because adsorption is exothermic, $K(T)$ decreases with increasing temperature. This property is critical in 4-zone TSMB-FC system because it enables simultaneous concentration of solutes in the higher temperature zones while regenerating the adsorbent.

2.2 SWD for non-isothermal systems

The SWD concept for 4-zone SMB system with linear isotherms was first introduced and thoroughly discussed by Ma and Wang (1997) for an isothermal system. To summarize their approach, the SWD method for non-ideal systems is derived from the mass balances for both the mobile phase (Eq. 13 in Appendix 1) and the pore phase

Table 1 a: System parameters and properties (Matz and Knaebel 1991) used in detailed simulations for both mass and energy balances to separate and concentrate *p*-xylene and toluene in silica gel; b: Numerical parameters used in the simulations

a

Column	L	30 cm
	I.D.	10 cm
	ε_i	0.43
	ε_T	0.715
Solid phase	d_p	0.335 mm
	ε_p	0.5
	ρ_S	1.05 g/mL
	C_{ps}	0.92 J/g/K
Liquid phase	ρ_L	0.684 g/mL
	C_{pL}	2.2439 J/g/K
	$k_{f,tol}$	5.565 min^{-1}
	$k_{f,px}$	4.712 min^{-1}
	$C_{F,tol}$	0.008 g/L
	$C_{F,px}$	0.008 g/L
	F	10 mL/min

b

Numerical parameter	Value
PDE discretization method	BUDS
No. of elements	40
Absolute tolerance	1.0E−09
Relative tolerance	1.0E−09
Initial step size	0.5
Minimum step size	0.5
Maximum step size	2.0

within zone j (Eq. 14) with mass transfer between phases determined from a linear driving force expression. The steady state solution of these equations must satisfy (15). The main difference between the isothermal and non-isothermal systems is the retention factor, $\delta_{i,j} = \varepsilon_p + (1 - \varepsilon_p)K(T)_{i,j}$, which varies in each zone of the non-isothermal system, because the $K(T)_{i,j}$ values depend on temperature.

The resulting SWD velocity of each zone in the 4-zone TSMB-FC system can be obtained by following a similar approach to Ma and Wang (1997) (Appendix 1). The resulting zone velocities are:

$$u_{o,1} = \left[1 + P\delta_{B,1}\right] u_{port} + \beta_1^B \left[\frac{D_{ax,B,1}}{L_1} + \frac{P\delta_{B,1}^2 u_{port}^2}{k_{f,B,1}L_1}\right] \quad (3a)$$

$$u_{o,2} = \left[1 + P\delta_{A,2}\right] u_{port} + \beta_2^A \left[\frac{D_{ax,A,2}}{L_2} + \frac{P\delta_{A,2}^2 u_{port}^2}{k_{f,A,2}L_2}\right] \quad (3b)$$

$$u_{o,3} = \left[1 + P\delta_{B,3}\right] u_{port} - \beta_3^B \left[\frac{D_{ax,B,3}}{L_3} + \frac{P\delta_{B,3}^2 u_{port}^2}{k_{f,B,3}L_3}\right] \quad (3c)$$

$$u_{o,4} = \left[1 + P\delta_{A,4}\right] u_{port} - \beta_4^A \left[\frac{D_{ax,A,4}}{L_4} + \frac{P\delta_{A,4}^2 u_{port}^2}{k_{f,A,4}L_4}\right] \quad (3d)$$

$$\text{where } \beta_j^i = \ln\left(\frac{c_{i,j,\max}}{c_{i,j,\min}}\right) \quad (3e)$$

The term β_j^i is the decay coefficient of solute i in zone j, which is defined as the natural log of the ratio of the highest and the lowest concentrations of i. A higher β value corresponds to higher product purity. As shown in Appendix 2, this parameter can also be determined from the yields of solute i, Y_i, using the component mass balances around the inlet and outlet ports (Eq. 19a, b). The final solutions for the decay coefficients are;

$$\beta_1^B = \ln\left(\frac{c_{E,B}}{c_{D,B}}\right) = \ln\left(\frac{\frac{Fc_{F,B}Y_B}{Q_1 - Q_2}}{\frac{Q_4}{Q_1}c_{R,B}}\right)$$

$$\beta_2^A = \ln\left(\frac{c_{Fb,A}}{c_{E,A}}\right) = \ln\left(\frac{\frac{Q_3\frac{Fc_{F,A}Y_A}{Q_3 - Q_4} - Fc_{F,A}}{Q_2}}{c_{E,A}}\right) \quad (4a, b)$$

$$\beta_3^B = \ln\left(\frac{c_{FP,B}}{c_{R,B}}\right) = \ln\left(\frac{\frac{Q_2\frac{Fc_{F,B}Y_B}{Q_1 - Q_2} + Fc_{F,B}}{Q_3}}{c_{R,B}}\right)$$

$$\beta_4^A = \ln\left(\frac{c_{R,A}}{c_{D,A}}\right) = \ln\left(\frac{\frac{Fc_{F,A}Y_A}{Q_3 - Q_4}}{\frac{Q_1}{Q_4}c_{E,A}}\right) \quad (4d, d)$$

$$c_{E,B} = \frac{Fc_{F,B}Y_B}{Q_1 - Q_2} \quad c_{R,A} = \frac{Fc_{F,A}Y_A}{Q_3 - Q_4} \quad (4e, f)$$

The $c_{k,i}$ is the concentration of solute i in the k port where the subscripts F, E, R, and D represent the feed, extract, raffinate, and desorbent ports, while $c_{FP,i}$ is the concentration of solute i after the feed port and $c_{Fb,i}$ is the concentration before the feed port. To ensure high purity and high EF, the concentration of solute A in extract, $c_{E,A}$, and that of solute B in raffinate, $c_{R,B}$, have to be small. The overall mass transfer coefficient, k_f, in (3) is the lumped mass transfer coefficient based on the linear driving force determined at the lowest temperature and assumed to be temperature independent. This assumption likely underestimates the mass transfer coefficient resulting in a more conservative design because k_f is expected to increase with increasing temperature. Once the zone velocities are determined through the SWD method, the port velocity, u_{port}, can be determined through the mass balance with the feed port, zone 2, and zone 3 as the control volume, and solving for u_{port}.

$$\frac{F}{\varepsilon_e S} = u_{o,3} - u_{o,2} \tag{5a}$$

$$a\,u_{port}^2 + b\,u_{port} + c = 0 \tag{5b}$$

where

$$a = \frac{\beta_{2,hot}^A P \delta_{A,2}^2}{k_{f,A,2} L_2} + \frac{\beta_{3,cold}^B P \delta_{B,3}^2}{k_{f,B,3} L_3} \tag{5c}$$

$$b = -P\left[\delta_{B,3} - \delta_{A,2}\right] \tag{5d}$$

$$c = \frac{Q_F}{\varepsilon_e S} + \beta_2^A \frac{D_{ax,A,2}}{L_2} + \beta_3^B \frac{D_{ax,.B,3}}{L_3} \tag{5e}$$

where F is the feed flow rate and S is the column cross-sectional area. The port switching time is defined by $t_{sw} = L/u_{port}$ and $Q_i = \varepsilon_e S u_{o,i}$. In solving (5b), the SWD method only has a meaningful solution when:

$$P^2\left[\delta_{B,3} - \delta_{A,2}\right]^2 - 4\left[\frac{\beta_2^A P \delta_{A,2}^2}{k_{f,A,2} L_2} + \frac{\beta_3^B P \delta_{B,3}^2}{k_{f,B,3} L_3}\right] \left[\frac{Q_F}{\varepsilon_e S} + \beta_2^A \frac{D_{ax,A,2}}{L_2} + \beta_3^B \frac{D_{ax,.B,3}}{L_3}\right] \geq 0 \tag{6}$$

Since the decay coefficients, β_j^i, in (4) depend on the zone flow rates, Q_j, this leads to the following iterative procedure:

1. Input the known parameters, such as the feed flow rate, feed concentration, the impurity concentrations in the extract and raffinate [$c_{E,A}$ and $c_{R,B}$ in (19)], and zone temperatures along with the parameters shown in Table 1.
2. Initial guess of the decay coefficients, $\beta_j^{i(0)}$.
3. Determine the zone velocities, which provide the flow rates, and the port velocity using (3) and (5), respectively.
4. Calculate $\beta_j^{i(1)}$ and see if $\beta_j^{i(1)} = \beta_j^{i(0)}$.
5. If yes, the output operating parameters are obtained.
6. If not, use direct substitution, set $\beta_j^{i(1)} = \beta_j^{i(0)}$ and return to step 3.
7. Continue until $\left|\beta_j^{i(1)} - \beta_j^{i(0)}\right| < 0.001$.

Obviously, other convergence methods can be used, but simple direct substitution is effective.

In deriving the SWD method equations, the density and heat capacities are assumed to be constant, thermal dispersion is assumed to be negligible, and temperature changes are assumed to be instantaneous. Although not strictly true, the last assumption causes little error because in dilute systems the thermal and solute wave velocities are decoupled and the thermal wave velocity is shown below (Wankat 1994),

$$u_{th} = \frac{\overline{u}_o}{1 + \frac{(1-\varepsilon_e)\varepsilon_p}{\varepsilon_e} + \frac{(1-\varepsilon_e)(1-\varepsilon_p)C_{p,s}\rho_s}{\varepsilon_e \rho_f C_{p,f}}} \tag{7}$$

The thermal wave is typically much faster than solute waves in liquid adsorption systems. The thermal wave velocity stems from an energy balance where the heat of adsorption and heat of mixing is ignored, and an adiabatic column is assumed. Less than one superficial column volume is sufficient for the column temperature to reach thermal equilibrium. In addition, if each zone has two or more columns, the first column in each zone is already at the right temperature; only the last column in each zone may be at the wrong temperature immediately after the switch of ports and heat exchangers. As shown in the Aspen simulation results in Sect. 3, thermal equilibrium is reached within a fraction of the switching time (<0.4 t_{sw}), and the assumption of instantaneous temperature change in the SWD method is justified.

2.3 Detailed simulations

In order to show that the SWD method results in optimum operating conditions and to explore the 4-zone TSMB-FC system profiles, detailed simulations using Aspen Chromatography 2006 software were performed until cyclic steady state was reached. All systems had 2 columns per zone. The two porosity mass balance model was used,

$$\varepsilon_e \frac{\partial c_i}{\partial t} + K_{di}(1-\varepsilon_e)\varepsilon_p \frac{\partial \overline{c}_{i,pore}}{\partial t} + (1-\varepsilon_e)(1-\varepsilon_p)\rho_S \frac{\partial \overline{q}_i}{\partial t} + \varepsilon_e \frac{\partial (u_o c_i)}{\partial z} = \varepsilon_e (D_{ax}) \frac{\partial^2 c_i}{\partial z^2} \tag{8}$$

where ρ_S is the solid phase density; u_o is the interstitial velocity of the mobile phase within the column; and D_{ax} is the axial diffusivity. The $\frac{\partial \overline{q}}{\partial t}$ term is defined by the linear lumped mass transfer parameter based on liquid phase concentrations.

$$\frac{\partial \overline{q}_i}{\partial t} = k_{f,i} a_p \left(c_i - c_i^*\right) \tag{9}$$

Combining (8) and (9) gives the linear lumped parameter kinetic model. The axial dispersion coefficient is estimated with the Chung-Wen correlation (1968).

The two porosity energy balance was solved for an adiabatic column.

$$\rho_L Cp_L \frac{\partial(\overline{u}_o T)}{\partial z} + \rho_L Cp_L \left[\varepsilon_e + (1-\varepsilon_e)\varepsilon_p\right] \frac{\partial T}{\partial t} + \rho_S Cp_S (1-\varepsilon_e)(1-\varepsilon_p) \frac{\partial T}{\partial t} = D_{ax,E}\, \rho_L Cp_L\, \varepsilon_e \frac{\partial^2 T}{\partial z^2} \quad (10)$$

where ρ_L and ρ_S are the liquid and solid phase density; C_{pL} and C_{pS} are the liquid and solid phase heat capacity, respectively; and $D_{ax,E}$ is the thermal axial dispersion coefficient. The energy balance in Aspen Chromatography simulations is decoupled from the mass balance for dilute solutions. The thermal wave travels much faster than the solute waves. Thus, although the change in temperature after port switching is not instantaneous, thermal equilibration is rapid.

To compare the performance of the 4-zone TSMB-FC system, we define an enrichment factor (EF_R or EF_E), which is the concentration ratio of the major component in the extract or the raffinate stream with respect to its feed concentration. A purity index (PI) is the average purity of the two major components in the extract and the raffinate stream,

$$EF_R = \frac{c_{R,A}}{c_{F,A}} \quad \text{and} \quad EF_E = \frac{c_{E,B}}{c_{F,B}} \quad PI = \frac{P_{R,A} + P_{E,B}}{2} \quad (11a, b)$$

where $c_{R,i}$, $c_{E,i}$, and $c_{F,i}$ are the concentrations of solute i in the raffinate, extract, and feed, respectively, and $P_{R,i}$ and $P_{E,i}$ are the purity of solute i in the raffinate and the extract, respectively.

3 Results and discussion

The SWD method was first tested for isothermal four-zone SMB systems with two columns per zone. The optimum operating condition (zone velocities and port switching time) was determined for arbitrary but low impurity concentrations in the product streams ($c_{R,B} = 0.0001$ and $c_{E,A} = 0.00001$). The SWD yields were determined from (19) based on the feed concentrations and feed flow rate in Table 1 and the specified impurity concentrations. The iteration procedure in the Theory section was used to find the port switching time, β values, and the velocities in the four zones for various temperatures. Simulations were run with these operating conditions to check the yields, the product purities, and the EFs (Table 2). The yield values calculated in the SWD vary from 97.97 to 98.23 % for B (p-xylene) and from 99.8 to 99.82 % for A (toluene). The variations are due to the different zone flow rates at the different temperatures. The yield values calculated by Aspen were within 0.5 % of those calculated in the SWD. The small differences could be due to the assumption of TMB in SWD, while the Aspen simulations used the periodic moving port systems. The agreement indicates that the SWD works well for the isothermal SMB systems. As expected, the 4-zone isothermal SMBs at different temperatures produce high-purity products ($P_i > 99$ %), but there is product dilution, D/F > 1.0.

This procedure was repeated with different zone temperatures to find the effects of temperature distribution on the 4-zone TSMB-FC performance (Tables 3, 4, 5). Since the flow rates were smaller in most of the non-isothermal SMB systems, slightly higher yields were calculated based on the same impurity concentrations in the two product streams, as expected from (19). The yield values in the SWD and those from Aspen simulations also agree to within 0.5 % as for isothermal systems.

The operating temperature of 25 °C was used as the base condition for non-isothermal operation of a 4-zone TSMB-FC in Table 3. As the temperatures for zone 1 and zone 2 were increased and that of zone 4 was decreased, the D/F

Table 2 Simulation results for isothermal 4-zone SMB

Temperature (°C)				Purity		Yield				EF		D/F
Zone 1	Zone 2	Zone 3	Zone 4	Extract (B)	Raffinate (A)	Extract (B)		Raffinate (A)		Extract (B)	Raffinate (A)	
				p-xylene	Toluene	SWD	Aspen	SWD	Aspen			
0	0	0	0	99.7	98.5	98.22	98.43	99.82	99.71	0.68	0.70	1.87
10	10	10	10	99.8	98.6	98.23	98.62	99.82	99.79	0.69	0.70	1.85
20	20	20	20	99.8	98.6	98.23	98.63	99.82	99.80	0.69	0.70	1.85
25	25	25	25	99.8	98.7	98.23	98.44	99.82	99.75	0.68	0.70	1.86
30	30	30	30	99.8	98.7	98.22	98.43	99.82	99.74	0.68	0.70	1.87
40	40	40	40	99.7	98.6	98.20	98.34	99.82	99.84	0.68	0.69	1.89
50	50	50	50	99.8	98.6	98.17	98.29	99.82	99.52	0.67	0.68	1.94
60	60	60	60	99.7	98.4	98.12	98.26	99.81	99.61	0.65	0.66	2.01
70	70	70	70	99.7	98.2	98.06	98.20	99.81	99.65	0.63	0.64	2.10
80	80	80	80	99.5	97.8	97.97	97.62	99.80	99.62	0.61	0.61	2.23

Table 3 Simulation results for 4-zone TSMB-FC system with $0 \leq D/F \leq 1$

Temperature (°C)				Purity		Yield				EF		D/F
Zone 1	Zone 2	Zone 3	Zone 4	Extract (B)	Raffinate (A)	Extract (B)		Raffinate (A)		Extract (B)	Raffinate (A)	
				p-xylene	Toluene	SWD	Aspen	SWD	Aspen			
35	25	25	25	99.8	98.6	98.14	98.58	99.95	99.85	2.30	0.67	0.92
35	30	25	25	99.8	99.1	98.81	98.97	99.93	99.83	1.83	1.05	0.50
35	30	25	20	99.8	99.3	99.15	99.33	99.93	99.73	1.84	1.47	0.22
38.83	30	25	20	99.8	99.3	99.16	99.35	99.96	99.81	1.48	3.07	0.00

Table 4 Simulation results for 4-zone TSMB-FC with $D/F < 0$ and $\Delta T_{cold} = 0$ for max EF_E

Temperature (°C)				Purity		Yield				EF		D/F
Zone 1	Zone 2	Zone 3	Zone 4	Extract (B)	Raffinate (A)	Extract (B)		Raffinate (A)		Extract (B)	Raffinate (A)	
				p-xylene	Toluene	SWD	Aspen	SWD	Aspen			
60	45	30	30	99.9	99.3	99.18	99.29	99.99	99.92	15.40	1.53	−0.28
60	45	20	20	99.9	99.5	99.36	99.50	99.99	99.91	25.35	1.97	−0.45
60	45	10	10	99.9	99.6	99.47	99.62	99.99	99.82	38.08	2.32	−0.55
60	45	0	0	99.9	99.7	99.53	99.71	99.99	99.90	57.75	2.68	−0.61

Table 5 Simulation results for 4-zone TSMB-FC with $D/F < 0$ and $\Delta T_{hot} = 0$ for max EF_R

Temperature (°C)				Purity		Yield				EF		D/F
Zone 1	Zone 2	Zone 3	Zone 4	Extract (B)	Raffinate (A)	Extract (B)		Raffinate (A)		Extract (B)	Raffinate (A)	
				p-xylene	Toluene	SWD	Aspen	SWD	Aspen			
60	60	40	30	99.9	99.7	99.66	99.68	99.95	99.74	2.41	3.65	−0.31
60	60	30	20	99.9	99.8	99.76	99.69	99.97	99.75	3.65	5.19	−0.53
60	60	20	10	99.8	99.8	99.83	99.81	99.98	99.65	5.33	7.26	−0.68
60	60	10	0	99.7	99.8	99.88	99.53	99.98	99.63	7.62	10.30	−0.78

value was reduced to smaller than 1. As a result, both the extract and raffinate products could be concentrated while maintaining the desired purity. Notice in the last case in Table 3, the D/F values was zero. This poses an interesting possibility to further increase *EF* by withdrawing desorbent from the SMB system (negative *D/F*) instead of introducing it for column regeneration.

Tables 4 and 5 show the zone temperature conditions allowing the 4-zone TSMB-FC system to be operated under negative *D/F* values. In Table 4, the zone 1 and zone 2 temperatures were fixed at 60 and 45 °C, respectively, while the zone 3 and zone 4 temperatures were operated such that $T_3 = T_4$ and varied between 30 and 0 °C. In Table 5, the zone 1 and zone 2 were both fixed at 60 °C, while zone 3 and zone 4 were operated such that T_3–$T_4 = 10$ °C and varied between 40 and 0 °C. Both the SWD and the simulation results show that the *D/F* values were negative, which means the desorbent can be withdrawn from the system. As the zone 3 and zone 4 temperatures were decreased, the enhancement factors, *EF*, for the extract and the raffinate were increased. Notice that when $T_3 = T_4$ (Table 4), the EF of the extract, EF_E, is greater than that of the raffinate, EF_R. However, EF_R was greater than EF_E when $T_1 = T_2$ (Table 5). This trend demonstrates two possible operations of the 4-zone TSMB-FC system; one is an operation that allows higher *EF* for the extract product and another that allows higher *EF* for raffinate product. For the former, the 4-zone TSMB-FC has to operate at the same temperature for zone 3 and zone 4 as shown in Table 4. For the latter, the system has to operate at the same temperature for zone 1 and zone 2 (Table 5).

To validate the aforementioned temperature effects and further confirm the accuracy of the SWD method, the predicted *EF* from the SWD method were compared with the simulation results and shown in Figs. 3 and 4. In SWD, once the operating parameters were successfully determined from the iterative procedure, the desired product concentration in the extract ($c_{E,B}$) and raffinate ($c_{R,A}$) were

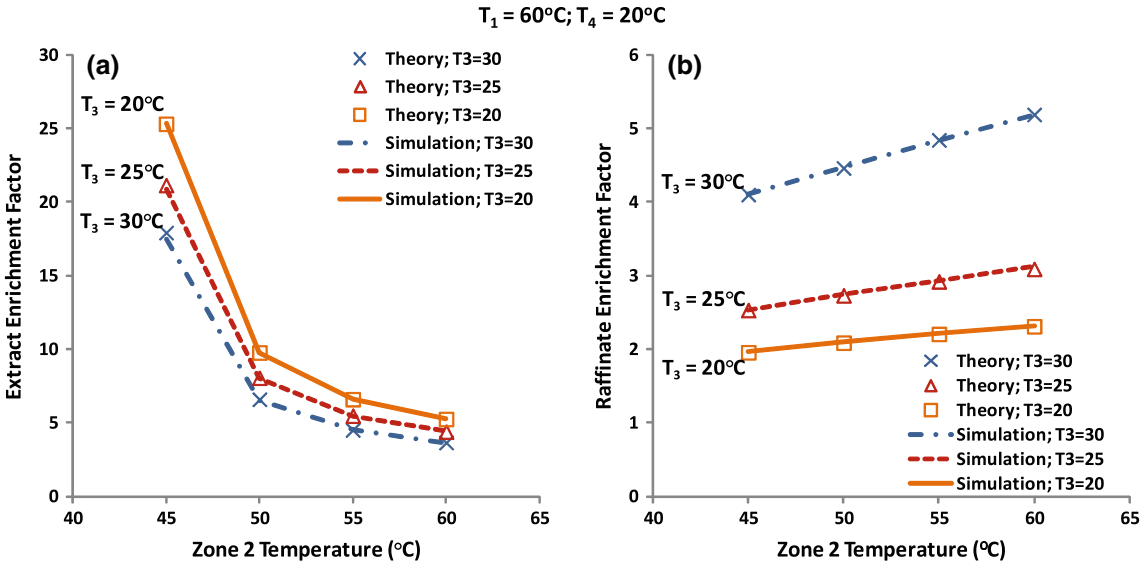

Fig. 3 SWD validation and EF simulation results of 4-zone TSMB-FC at varying T_2, T_3 and constant $T_1 = 60$ °C, $T_4 = 20$ °C for **a** extract product, **b** raffinate product

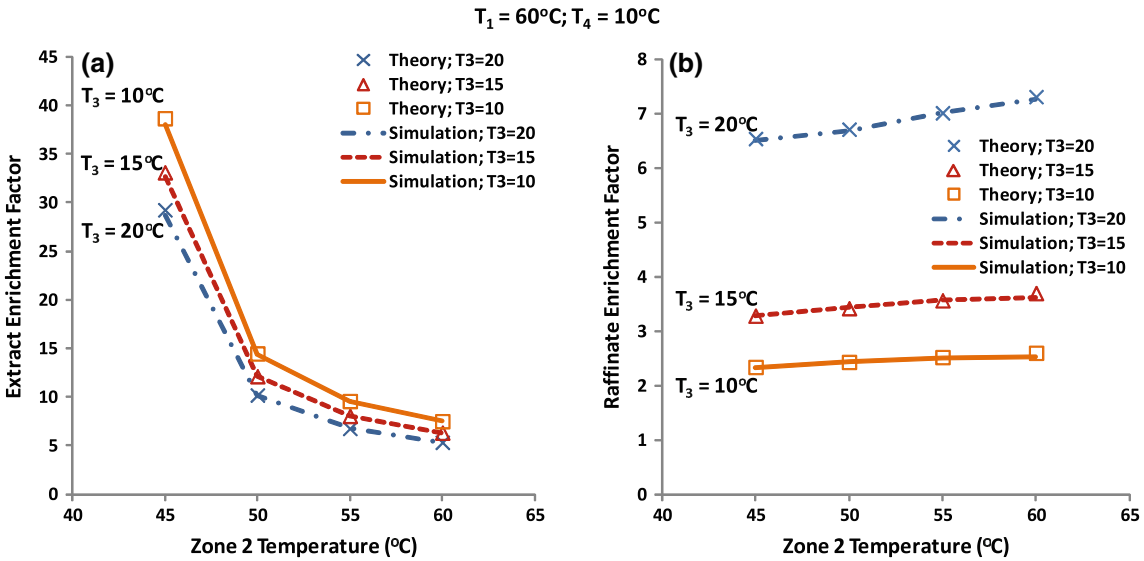

Fig. 4 SWD validation and EF simulation results of 4-zone TSMB-FC at varying T_2, T_3 and constant $T_1 = 60$ °C, $T_4 = 10$ °C for **a** extract product, **b** raffinate product

easily obtained from the yield equation (4e) and (4f), and the predicted *EF* values were obtained using (11a). The results in Figs. 3 and 4 depict the *EF* results at varying intermediate zone 2 and 3 temperatures while keeping the cold zone 4 temperature constant at 20 and 10 °C, respectively, and the hot zone 1 at 60 °C for both cases (Figs. 3a and 4a are for concentrating the extract product, and Figs. 3b and 4b are for concentrating the raffinate product). The SWD results at different temperatures are in very good agreement with the simulation results, indicating that the SWD method is an accurate and reliable tool for determining the optimal operating conditions for the 4-zone TSMB-FC.

Figure 3 further confirms that the maximum EF_E is obtained when the temperature difference in the hot zones (zone 1 and zone 2), $\Delta T_{hot} = T_1 - T_2$, is the highest and that in the cold zones (zone 3 and zone 4), $\Delta T_{cold} = T_3 - T_4$, is the lowest or at the same temperature ($\Delta T_{cold} = 0$ °C). The maximum $EF_E = 25$ is obtained for $T_1 = 60$ °C, $T_2 = 45$, $T_3 = 20$ °C, and $T_4 = 20$ °C. On the other hand, the maximum EF_R is obtained when $\Delta T_{hot} = T_1 - T_2$ is the lowest or at the same temperature

and $\Delta T_{cold} = T_3 - T_4$ is the highest. The maximum $EF_R = 5$ for $T_1 = 60$ °C, $T_2 = 60$, $T_3 = 30$ °C, and $T_4 = 20$ °C is obtained (Tables 4, 5). The SWD restriction shown in (6) requires maximum temperature differences of $\Delta T_{hot} = 15$ °C and $\Delta T_{cold} = 10$ °C.

As the temperature of the cold zones (zones 3 and 4) are lowered by 10 °C (Fig. 4), more solute will adsorb in the cold zones and more will desorb in the hot zones, resulting in higher EF. For the extract, the maximum $EF_E = 38$ is obtained for $T_1 = 60$ °C, $T_2 = 45$, $T_3 = 10$ °C, and $T_4 = 10$ °C (Fig. 4a). The maximum $EF_R = 7$ is obtained for the case $T_1 = 60$ °C, $T_2 = 60$, $T_3 = 20$ °C, and $T_4 = 10$ °C (Fig. 4b).

Increasing the overall temperature difference between the hot and cold zones reduces the *D/F* ratio and improves the EF (with constant $c_{R,B} = 0.0001$ and $c_{E,A} = 0.00001$ for all the runs). Figure 4 shows the same trend as Fig. 3 in terms of ΔT_{hot} and ΔT_{cold} for maximizing *EF* of a specific product. Similar trend is also observed for maximizing the extract and raffinate purities (Figs. 5, 6) except that both product purities are improved when $\Delta T_{hot} = T_1 - T_2$ is highest. For example, the maximum purities of the extract products in Figs. 5 and 6 are both 99.9 % obtained when $\Delta T_{hot} = T_1 - T_2$ is highest (15 °C). The raffinate products, on the other hand, have a maximum purity of 99.9 % (ΔT_{hot} = maximum = 15 °C; ΔT_{cold} = maximum = 10 °C). Figure 7 shows the purity indices (*PI*) for the first and second cases. The *PI* results follow the behaviour of the raffinate product purity results very closely where the maximum purity index can be obtained at maximum ΔT_{hot} and ΔT_{cold}.

Assuming that maximum EF_E is desired, additional simulations were performed with temperature variation on the cold zones 3 and 4 (at $\Delta T_{cold} = 0$) while keeping the $T_1 = 60$ °C and $T_2 = 45$ °C. The simulation results are shown in last run of Table 4. As expected, the results are consistent with the previous prediction where higher temperature gradient between the hot and cold zones leads to lower *D/F* ratio and higher *EF* for both the extract and raffinate products. Simulations were also performed for the case with the higher EF_R. The results for $\Delta T_{hot} = 0$ °C at $T_1 = T_2 = 60$ °C while changing the temperatures of zones 3 and 4 are shown in Table 5. The results show that increasing the temperature difference between the hot and cold zones not only improves the *EF* for the extract product but also improves the *EF* for the raffinate product.

In an already existing system with fixed columns, packing, and particle size, the mass transfer and dispersion coefficients are constant. Thus, the easiest and most flexible variables for design improvement besides temperature are the flow rates and port switching, which are related to the decay coefficient, β_j^i, that is dependent on the specified impurity concentrations (refer to (3) and (4)). All the runs performed up to this point were at constant $c_{R,B} = 0.0001$ and $c_{E,A} = 0.00001$. Lower $c_{R,B}$ means higher concentration ratio of the high affinity solute *B* resulting in higher raffinate product purity. The same trend also applies when $c_{E,A}$ is decreased where concentration ratio of solute *A* is higher. Therefore, product purity can be increased by lowering the $c_{R,B}$ and $c_{E,A}$ values while the opposite also holds as shown in runs 2–5 in Table 6 where the $X_{R,B}$ and $X_{E,A}$ is defined as the ratio of the new and old $c_{R,B}$ and $c_{E,A}$, respectively.

$$X_{R,B} = \frac{c_{R,B,new}}{c_{R,B,base}} \quad X_{E,A} = \frac{c_{E,A,new}}{c_{E,A,base}} \qquad (12a, b)$$

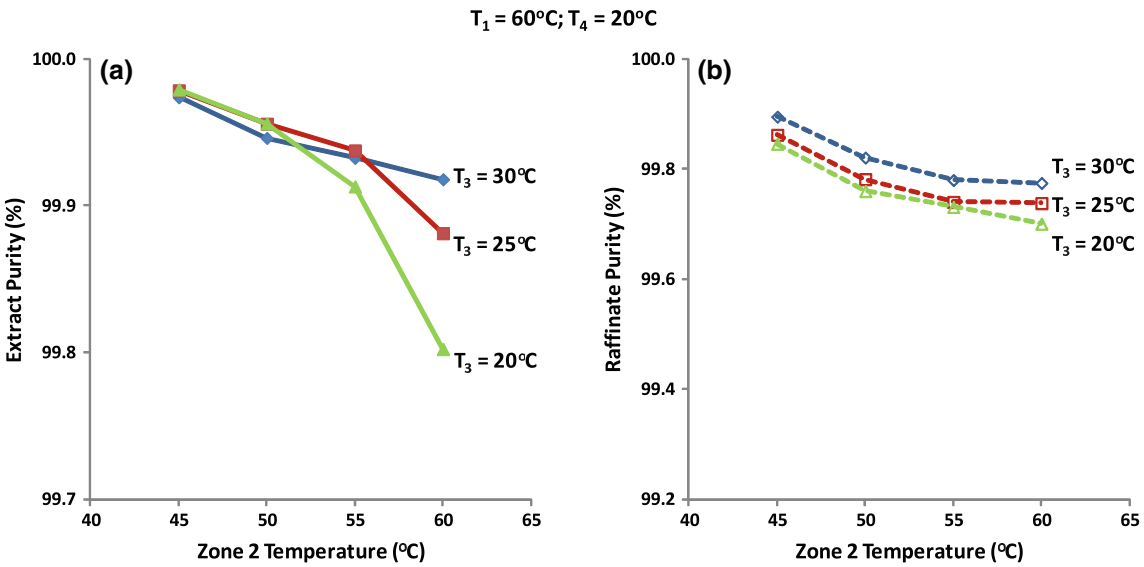

Fig. 5 Product purity simulation results for 4-zone TSMB-FC at varying T_2, T_3 and constant $T_1 = 60$ °C, $T_4 = 20$ °C for **a** extract product, **b** raffinate product

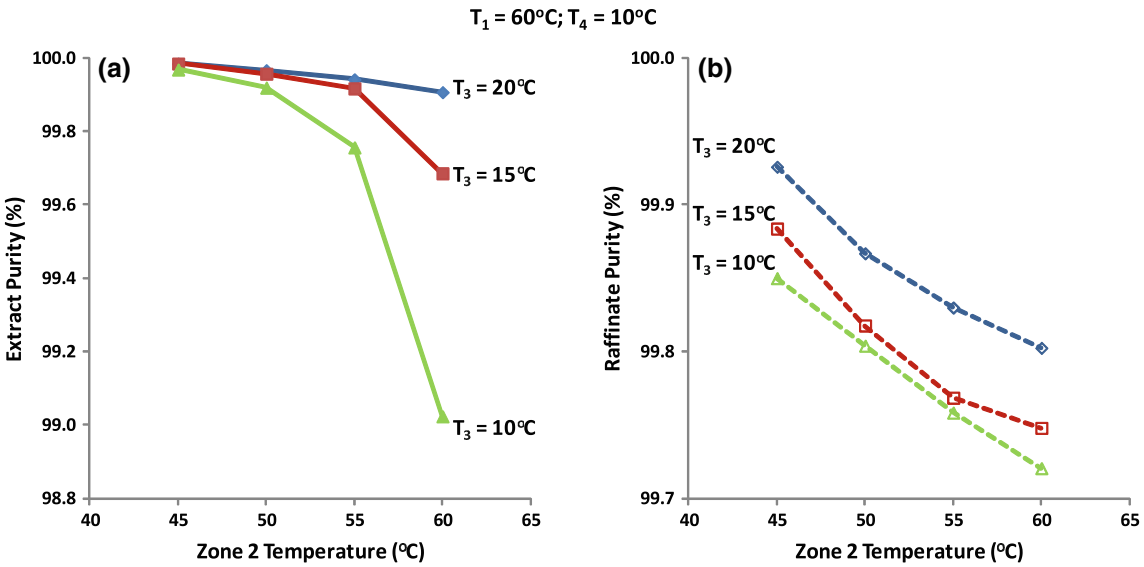

Fig. 6 Product purity simulation results for 4-zone TSMB-FC at varying T_2, T_3 and constant $T_1 = 60$ °C, $T_4 = 10$ °C for **a** extract product, **b** raffinate product

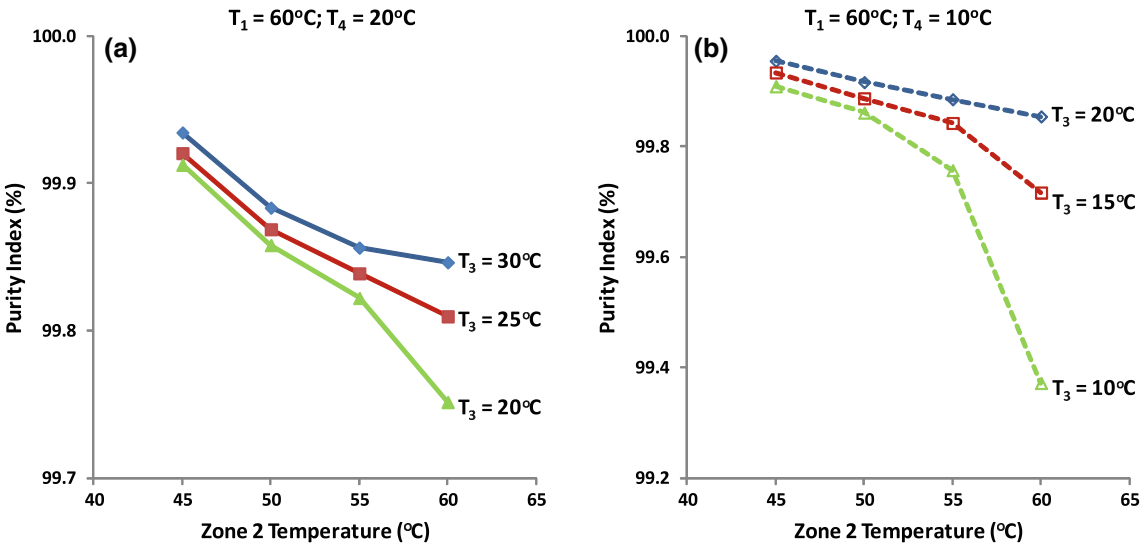

Fig. 7 Product purity index simulation results for 4-zone TSMB-FC at varying T_2, T_3 for constant **a** $T_1 = 60$ °C, $T_4 = 20$ °C, **b** $T_1 = 60$ °C, $T_4 = 10$ °C

However, higher product purity for the 4-zone TSMB-FC does not necessarily mean that the EF will also improve.

According to (3) and (4), the *EF* value for the 4-zone TSMB-FC highly depends on the flow rates in each zone, Q_i. Flow rates can be adjusted to retain purity levels by varying the decay coefficients, β_j^i. Note from (4) that β_j^i is a function of the product yields, Y_i, which was obtained from $c_{R,B}$ and $c_{E,A}$. Thus, the *EF*, can be fine-tuned depending on the product yields or the $c_{R,B}$ and $c_{E,A}$. The simulation results for the effects of yields and, thus, the $c_{R,B}$ and $c_{E,A}$ are shown in Table 6 with run 1 ($c_{R,B} = 0.0001$ and $c_{E,A} = 0.00001$) as the base case. If the maximum EF_E is desired, the denominator term of (4e), $Q_1 - Q_2$ (or Q_E), needs to be minimized. One approach to minimize Q_E is by decreasing Q_1. To decrease Q_1, one must decrease the yield of B (Y_B) or increase the impurity concentration of B in the raffinate ($c_{R,B}$). From this Y_B or $c_{R,B}$ manipulation, the β_1^B is decreased resulting in a lower flow rates in zone 1 (Q_1) and thus a higher EF_E (Eq. 4e). An alternative approach is to increase Q_2 by increasing the yield of A (Y_A) or decreasing the impurity concentration of A in the raffinate ($c_{E,A}$). As Y_A is increased, the β_2^A increased and, thus, the flow rates in zone 2 (Q_2) are increased. The simulation results for improving EF_E are shown in runs 3, 4, 6, and 7 in Table 6.

Table 6 Product yields sensitivity analysis of the simulations results by varying $X_{R,B} = c_{R,B,new}/c_{R,B,base}$ and $X_{E,A} = c_{E,A,new}/c_{E,A,base}$ on the 4-zone TSMB-FC *EFs* with $T_1 = 60$ °C; $T_2 = 45$ °C; $T_3 = 10$ °C; $T_4 = 10$ °C

Run	$Y_{B,SWD}$ ($Y_{B,Aspen}$)	$Y_{A,SWD}$ ($Y_{A,Aspen}$)	$X_{R,B}$	$X_{E,A}$	β_1	β_2	β_3	β_4	Purity		EF		D/F
									Extract (B)	Raffinate (A)	Extract (B)	Raffinate (A)	
1	99.47 (*99.62*)	99.99 (*99.92*)	1	1	7.48	8.13	7.19	8.09	100.0	99.9	38.08	2.32	-0.55
2	99.99 (*99.97*)	99.99 (*99.92*)	0.10	1	9.60	8.16	9.32	8.11	100.0	100.0	31.70	2.40	-0.55
3	94.50 (*94.69*)	99.99 (*99.92*)	10	1	5.33	8.11	5.04	8.09	100.0	99.6	46.11	2.30	-0.55
4	99.47 (*99.62*)	99.999 (*99.98*)	1	0.10	7.67	10.39	7.38	10.36	100.0	99.9	46.43	2.28	-0.54
5	99.47 (*99.62*)	99.48 (99.55)	1	10	7.31	5.88	7.03	5.84	99.9	99.9	32.88	2.41	-0.56
6	94.50 (*94.69*)	99.999 (*99.98*)	10	0.10	5.57	10.37	5.27	10.35	100.0	99.7	56.94	2.24	-0.54
7	86.56 (*86.75*)	99.999 (*99.99*)	100	0.01	3.36	12.61	3.05	12.60	100.0	99.2	79.95	2.16	-0.53
8	99.999 (*99.99*)	99.42 (*99.50*)	0.01	100	11.50	3.67	11.25	3.61	99.5	100.0	21.72	2.59	-0.58

(Run 1 serves as the base case with $c_{R,B,base} = 0.0001$ and $c_{E,A,base} = 0.00001$)

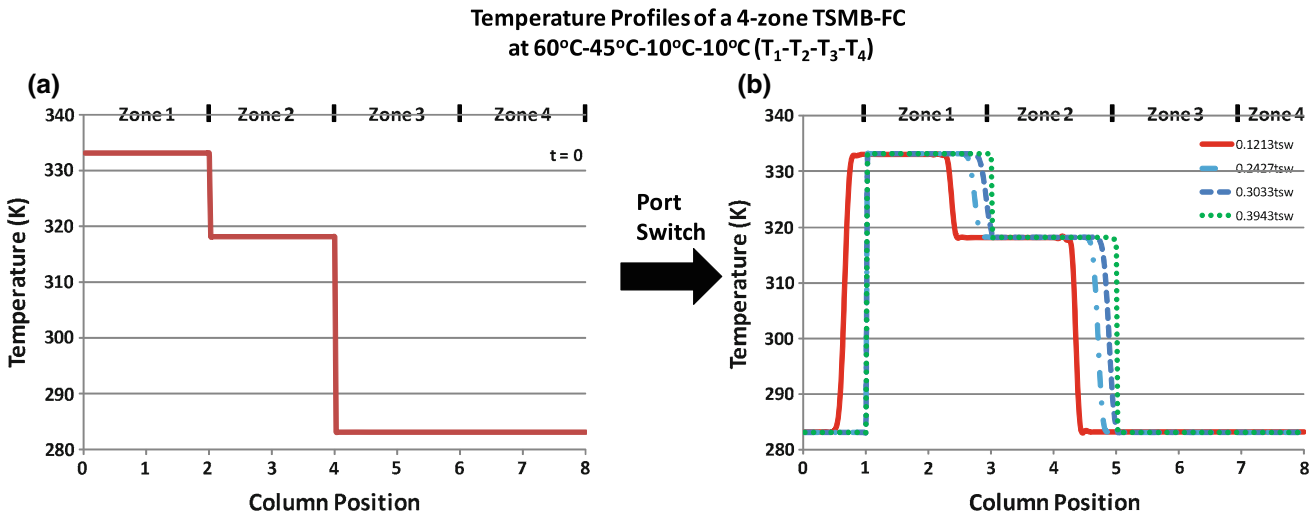

Fig. 8 Temperature profiles of a 4-zone TSMB-FC with 2 columns per zone at cyclic steady state at $T_1 = 60$ °C, $T_2 = 45$ °C, $T_3 = 10$ °C, $T_4 = 10$ °C

On the other hand, if higher EF_R is preferred, the Y_A needs to be reduced and/or the Y_B has to be increased as shown in runs 2, 5, and 8 in Table 6.

These results assume that the isotherms are strictly linear and independent. Thus, there is no limitation in concentrating the products. Obviously, there will be a point where the isotherm is no longer linear. Once the isotherm begins to behave non-linearly, the EFs of the desired product will be limited and a maximum value of *EF* is expected after which the concentrating ability will decrease as feed concentration is increased. In the non-linear isotherm region the *D/F* ratio is expected to be higher than in the linear region. The TSMB-FC analysis determines the maximum concentrating ability because the SWD method determines the minimum required *D/F* for given column configuration, temperature, feed flow rate, and feed concentration.

To understand the fractionation and concentration processes of the TSMB-FC, the temperature and concentration profiles for the temperatures $T_1 = 60$ °C, $T_2 = 45$ °C, $T_3 = 10$ °C, and $T_4 = 10$ °C are shown in Figs. 8 and 9. The temperature profile shown in Fig. 8 starts from $t = 0$ until it reaches thermal equilibrium. Because the thermal wave is much faster than the concentration waves, temperature equilibration is achieved relatively quickly, $t < 0.4\ t_{sw}$, allowing good column utilization and more time for each zone to perform its respective role. This rapid temperature equilibrium behavior is consistent with the condition $u_{th} > u_{S,A} > u_{S,B}$ shown in Table 7, which is typical in dilute liquid systems.

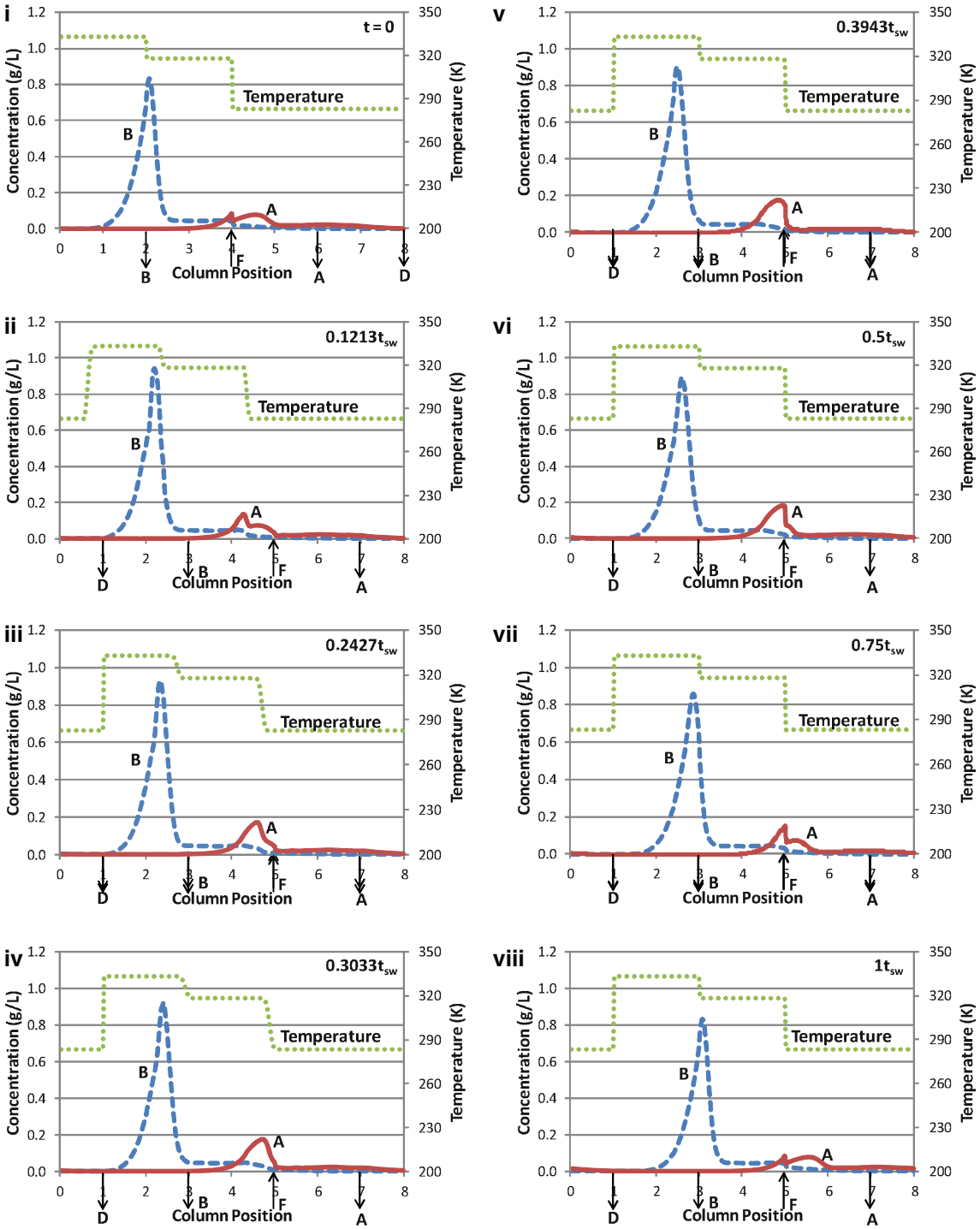

Fig. 9 Column temperature and concentration profiles at cyclic steady state of a 4-zone TSMB-FC operation with 2 columns per zone that focuses on maximizing the concentration of the extract product

The cyclic steady state concentration profiles for maximizing the *EF* of the extract product are shown in Fig. 9. It takes about 40 cycles for the TSMB-FC to reached cyclic steady state. These are the profiles as the temperature is equilibrating and after thermal equilibrium is reached. The snapshots show the profiles at different times starting from the beginning of the cycle at t = 0, and collectively they illustrate the progression of the solute waves for one full cycle. After port switching, the column temperatures begin to change to its respective temperature, which also result in the equilibration of the concentration profiles. As the temperature equilibrates (0.3943 t_{sw}), the shape of the

Table 7 Thermal wave and concentration wave velocities for 4-zone TSMB-FC at 60–45–10–10 °C (T_1–T_2–T_3–T_4) with t_{sw} = 817.78 min

Zones	Q_i (mL/min)	v_i (cm/min)	uth (cm/min)	$u_{s,A}$ (cm/min)	$u_{s,B}$ (cm/min)
1	7.312	0.217	0.104	0.047	0.037
2	7.054	0.209	0.100	0.037	0.029
3	17.054	0.505	0.243	0.046	0.035
4	12.800	0.379	0.182	0.035	0.026

concentration profile stabilizes and the focused solute bands then migrates toward the outlet port until the end of the step. The assumption of instantaneous temperature change in the SWD method overestimates the maximum concentration of the solutes resulting in a more conservative operating condition.

4 Conclusion

The SWD method was successfully modified to design a non-isothermal 4-zone SMB system for simultaneous fractionation and concentration (4-zone TSMB-FC) of two solutes for systems with linear isotherms and significant mass transfer effects. For a specified system configuration and temperature distribution in a 4-zone TSMB-FC, the modified SWD method enables the optimization of the flow rates and switching time to obtain the maximum productivity and minimal solvent consumption without trial-and-error simulations. For a dilute feed, a 4-zone TSMB-FC can significantly reduce the solvent required while improving the purity and *EF* of both the extract and raffinate products. The *EF* values obtained from the SWD method agree closely with those from the detailed Aspen Chromatography simulations. The SWD method correctly predicted that withdrawal of the desorbent (negative *D/F* ratios) further increases the EFs. Therefore, for a dilute feed it is possible to produce two pure products plus pure desorbent from a 4-zone TSMB-FC system. A detailed study of the temperature and concentration profiles shows that temperature equilibration occurs at less than $0.4t_{sw}$ and the concentration profiles are stabilized once temperature equilibrium is reached. The key parameters that control the EFs and purities of the 4-zone TSMB-FC are the temperature difference between zones 1 and 2, ΔT_{hot}, the temperature difference between zones 3 and 4, ΔT_{cold}, and the yields of the two solutes or the impurity concentrations in the products. In a standard isothermal SMB system, the highest cost is usually the energy consumption for desorbent recovery using either evaporators or distillation. Desorbent recovery cost will be significantly reduced for the 4-zone TSMB-FC system since it is able to recover desorbent and concentrate the solutes.

Acknowledgments Support from Purdue University is gratefully acknowledged. The authors are thankful to Dr. Anand Venkatesan and Mr. George Weeden from Purdue University for their helpful discussions and suggestions.

Appendix 1: Derivation of SWD equation

The mass balance equations for solutes in the mobile phase and pore phase within zone *i* shown in the equations below are used in deriving the mathematical model for the Linear, Non-Ideal SWD method (Ma and Wang 1997).

$$\frac{\partial c_{bi}}{\partial t} = D_{ax,i,j}\frac{\partial^2 c_{bi}}{\partial x^2} - \bar{u}_{o,j}\frac{\partial c_{bi}}{\partial x} - Pk_{f,i,j}\left(c_{bi} - c_i^*\right) \tag{13a}$$

$$\bar{u}_{o,j} = u_{o,j} - u_{port} \tag{13b}$$

$$\varepsilon_p\frac{\partial c_i^*}{\partial t} + \left(1-\varepsilon_p\right)\frac{\partial q_i^*}{\partial t} = k_{f,i,j}\left(c_{bi} - c_i^*\right) + u_{port}\varepsilon_p\frac{\partial c_i^*}{\partial x} + \left(1-\varepsilon_p\right)u_{port}\frac{\partial q_i^*}{\partial x} \tag{14}$$

where c_{bi} and c_i^* are the concentration of solute *i* in the mobile and pore phase, respectively; $D_{ax,i,j}$ is the axial dispersion coefficient of solute *i* in zone *j*; $\bar{u}_{o,j}$ is the interstitial velocity of the mobile phase in the axial direction; $u_{o,j}$ is the linear velocity in zone *j* that controls the propagation of the concentration waves relative to the solid phase; *P* is the bed phase ratio defined by $\frac{(1-\varepsilon_e)}{\varepsilon_e}$; $k_{f,i,j}$ is the mass transfer coefficient of solute *i* in zone *j*; u_{port} is the port velocity; and ε_p is the intra-particle void fraction.

The steady state solution to (13) and (14) in each zone must satisfy:

$$\left(D_{ax,i,j} + P\frac{\left(u_{port}\delta_i\right)^2}{k_{f,i,i}}\right)\frac{d^2C_{bi}}{dx^2} + \left[u_{port}(1+P\delta_i) - u_{o,j}\right]\frac{dC_{bi}}{dx} = 0 \tag{15}$$

where δ_i is the retention factor of solute *i* defined by $\delta_i = \varepsilon_p + (1-\varepsilon_p)K_i$; and K_i is the linear isotherm equilibrium constant. Remember that zones 1 and 2 desorbs solute *B* and *A*, respectively, while zones 3 and 4 adsorbs solute *B* and *A*, respectively. Using the feed port

(x = 0) as the reference point, the steady-state equation for solute A in zone 2 can be solved by rearranging (15) with the following boundary conditions:

$$\left[u_{o,2} - \left(1 + P\delta_{A,hot}\right)u_{port}\right]\frac{dC_{b,A}}{dx} = \left(D_{ax,A,2} + P\frac{\left(u_{port}\delta_{A,hot}\right)^2}{k_{f,A,2}}\right)\frac{d^2C_{b,A}}{dx^2} \quad (16a)$$

$$C_{b,A} = 0 \text{ at } x = -\infty \quad (16b)$$

$$C_{b,A} = C_{s,A} \text{ at } x = 0 \quad (16c)$$

The solution to (16) is shown in (3b).

In addition, the steady-state equation for solute B in zone 3 can also be solved using the following boundary conditions:

$$\left[u_{o,3} - \left(1 + P\delta_{B,cold}\right)u_{port}\right]\frac{dC_{b,B}}{dx} = \left(D_{ax,B,3} + P\frac{\left(u_{port}\delta_{B,cold}\right)^2}{k_{f,B,3}}\right)\frac{d^2C_{b,B}}{dx^2} \quad (17a)$$

$$C_{b,B} = 0 \text{ at } x = \infty \quad (17b)$$

$$C_{b,B} = C_{s,B} \text{ at } x = 0 \quad (17c)$$

The solution to (17) is shown in (3c). The velocities of zones 1 and 4 can also be derived using a similar approach where zones 1 and 4 will be solved using solute B and A, respectively. The overall zone velocity equation results are shown in (3).

Appendix 2: Derivation of decay coefficients of the SWD equation

The decay coefficients, β_j^i, for the SWD equations (3) is defined by the natural log of the ratio of the highest and lowest concentration of solute i in zone j. However, since the concentrations of the solutes inside the columns in each zone is unknown a priori, it is necessary to estimate the decay coefficients for the standing wave concentrations in each zone. One approach to do this is to link the concentration wave to the yield of each component through a simple mass balance of the inlet and outlet ports. The decay coefficient equations for each zone based on the concentration waves are as follows;

$$\beta_1^B = \ln\left(\frac{c_{E,B}}{c_{D,B}}\right) \quad \beta_2^A = \ln\left(\frac{c_{Fb,A}}{c_{E,A}}\right) \quad (18a, b)$$

$$\beta_3^B = \ln\left(\frac{c_{FP,B}}{c_{R,B}}\right) \quad \beta_4^A = \ln\left(\frac{c_{R,A}}{c_{D,A}}\right) \quad (18c, d)$$

where $c_{k,i}$ is the concentration of solute i in the k port where the subscripts F, E, R, and D represents the feed, extract, raffinate, and desorbent ports while $c_{FP,i}$ is the concentration of solute i after the feed port.

The yield of each component is defined by the ratio of the amount product produced in the outlet port and the amount of feed entering the system.

$$Y_A = \frac{c_{R,A}Q_R}{Fc_{F,A}} = 1 - \frac{c_{E,A}Q_E}{Fc_{F,A}} \quad Y_B = \frac{c_{E,B}Q_E}{Fc_{F,B}} = 1 - \frac{c_{R,B}Q_R}{Fc_{F,B}} \quad (19a, b)$$

where $Q_R = Q_3 - Q_4$ and $Q_E = Q_1 - Q_2$. By substituting Q_R and Q_E, and rearranging (B2) and solving for $c_{E,B}$ and $c_{R,A}$, the following equations are obtained.

$$c_{E,B} = \frac{Fc_{F,B}Y_B}{Q_1 - Q_2} \quad c_{R,A} = \frac{Fc_{F,A}Y_A}{Q_3 - Q_4} \quad (20a, b)$$

Next, the mass balance needed for solute A and B around both the raffinate and extract port are:

Solute A:

$$Q_2c_{Fb,A} + Fc_{F.A} = Q_3c_{R.A} \quad Q_4c_{D,A} = Q_1c_{E,A} \quad (21a, b)$$

Solute B:

$$Q_3c_{FP,B} = Q_2c_{E.B} + Fc_{F.B} \quad Q_1c_{D,B} = Q_4c_{R,B} \quad (22a, b)$$

The four equations are used to express the four unknown concentrations, $c_{Fb,A}$, $c_{FP,B}$, $c_{D,A}$, and $c_{D,B}$. Rearrangement of (B4) and (B5), and substituting these equations along with (B3) into (B1), the overall decay coefficient expression in terms of yield and zone flow rates are obtained and shown in (4).

References

Abunasser, N., Wankat, P.C.: Improving the performance of one column analogs to SMBs. AIChE J. **52**(7), 2461–2472 (2006)

Abunasser, N., Wankat, P.C., Kim, Y.S., Koo, Y.M.: One-column chromatograph with recycle analogous to a four-zone simulated moving bed. Ind. Eng. Chem. Res. **42**(21), 5268–5279 (2003)

Azevedo, D.C.S., Rodrigues, A.E.: Fructose–glucose separation in a SMB pilot unit: modeling, simulation, design, and operation. AIChE J. **47**(9), 2042–2051 (2001)

Beste, Y.A., Lisso, M., Wozny, G., Arlt, W.: Optimization of simulated moving bed plants with low efficient stationary phases: separation of fructose and glucose. J. Chromatogr. **A868**(2), 169–188 (2000)

Broughton, D.B., Carson, D.B.: The molex process. Pet. Refin. **38**(4), 130–134 (1959)

Broughton, D.B., Neuzil, R.W., Pharis, J.M., Brearley, C.S.: The Parex process for recovering paraxylene. Chem. Eng. Prog. **66**(9), 70–75 (1970)

Ching, C.B., Ruthven, D.M.: Experimental study of a simulated counter-current adsorption system—IV. Non-isothermal operation. Chem. Eng. Sci. **41**(12), 3063–3071 (1986)

Chung, S.F., Wen, C.Y.: Longitudinal, dispersion of liquid flowing through fixed and fluidized beds. AIChE J. **14**(6), 857–866 (1968)

Francotte, E.R., Richert, P.: Applications of simulated moving-bed chromatography to the separation of the enantiomers of chiral drugs. J. Chromatogr. **A769**(1), 101–107 (1997)

Guest, D.W.: Evaluation of simulated moving bed chromatography for pharmaceutical process development. J. Chromatogr. **A760**(1), 159–162 (1997)

Hritzko, B.J., Xie, Y., Wooley, R.J., Wang, N.H.L.: Standing wave design of tandem SMB for linear multicomponent systems. AIChE J. **48**(12), 2769–2787 (2002)

Jin, W., Wankat, P.C.: Thermal operation of four-zone simulated moving beds. Ind. Eng. Chem. Res. **46**(22), 7208–7220 (2007)

Jin, W., Wankat, P.C.: Two-zone SMB process for binary separation. Ind. Eng. Chem. Res. **44**(5), 1565–1575 (2005)

Keßler, L.C., Seidel-Morgenstern, A.: Improving performance of simulated moving bed chromatography by fractionation and feed-back of outlet streams. J. Chromatogr. **A1207**(1–2), 55–71 (2008)

Kim, J.K., Abunasser, N., Wankat, P.C.: Thermally assisted simulated moving bed systems. Adsorption **11**(1), 579–584 (2005)

Kim, J.K., Zang, Y., Wankat, P.C.: Single-cascade simulated moving bed systems for the separation of ternary mixtures. Ind. Eng. Chem. Res. **42**(20), 4849–4860 (2004)

Lee, J.W., Wankat, P.C.: Thermal simulated moving bed concentrator. Chem. Eng. J. **166**(2), 511–522 (2011)

Lee, K.N.: Two-section simulated moving bed process. Sep. Sci. Technol. **35**(4), 519–534 (2000)

Ludemann-Hombourger, O., Nicoud, M., Bailly, M.: The "VARICOL" process: a new multicolumn continuous chromatographic process. Sep. Sci. Technol. **35**(12), 1829–1862 (2000)

Ma, Z., Wang, N.H.L.: Standing wave analysis of SMB chromatography: linear Systems. AIChE J. **43**(10), 2488–2508 (1997)

Matz, M.J., Knaebel, K.S.: Recycled thermal swing adsorption: applied to separation of binary and ternary mixtures. Ind. Eng. Chem. Res. **30**(5), 1046–1054 (1991)

Mazzotti, M., Storti, G., Morbidelli, M.: Optimal operation of simulated moving bed units for nonlinear chromatographic separations. J. Chromatogr. **A769**(1), 3–24 (1997)

Migliorini, C., Mazzotti, M., Morbidelli, M.: Continuous chromatographic separation through simulated moving bed under linear and nonlinear conditions. J. Chromatogr. **A827**(2), 161–173 (1998)

Migliorini, C., Wendlinger, M., Mazzotti, M.: Temperature gradient operation of a simulated moving bed unit. Ind. Eng. Chem. Res. **40**(12), 2606–2617 (2001)

Murthy, D.S., Sivakumar, S.V., Kant, K., Rao, D.P.: Process intensification in a "simulated moving-bed" heat regenerator. J. Heat Transf. **130**(9), 1–091801 (2008)

Negawa, M., Shoji, F.: Optical resolution by simulated moving-bed adsorption technology. J. Chromatogr. **A590**(1), 113–117 (1992)

Nicolaos, A., Muhr, L., Gotteland, P., Nicoud, R.M., Bailly, M.: Application of equilibrium theory to ternary moving bed configurations (four + four, five + four, eight and nine zones): i. Linear case. J. Chromatogr. **A908**(1–2), 71–86 (2001)

Pais, L., Loureiro, J.M., Rodrigues, A.E.: Modeling strategies for enantiomers separation by SMB chromatography. AIChE J. **44**(3), 561–569 (1998)

Paredes, G., Rhee, H.K., Mazzotti, M.: Design of simulated-moving-bed chromatography with enriched extract operation (EE-SMB): Langmuir isotherms. Ind. Eng. Chem. Res. **45**(18), 6289–6301 (2006)

Schramm, H., Kaspereit, M., Kienle, A., Seiderl-Morgenstern, A.: Simulated moving bed process with cyclic modulation of the feed concentration. J. Chromatogr. **A1006**(1–2), 77–86 (2003)

Sivakumar, S.V., Rao, D.P.: Adsorptive separation of gas mixtures: mechanistic view, sharp separation, and process intensification. Chem. Eng. Proc. **53**, 31–52 (2012)

Storti, G., Mazzotti, M., Morbidelli, M., Carra, S.: Robust design of binary countercurrent adsorption separation process. AIChE J. **39**(3), 471–492 (1993)

Wankat, P.C.: Rate-Controlled Separations, Chapt. 6. Chapman & Hall, Glasgow (1994)

Wankat, P.C.: Separation Process Engineering: Includes Mass Transfer Analysis, 3rd edn., Chapt. 18. Pearson Education Inc., Upper Saddle River (2012)

Wooley, R., Ma, Z., Wang, N.H.L.: A nine-zone simulating moving bed for the recovery of glucose and xylose from biomass hydrolyzate. Ind. Eng. Chem. Res. **37**(9), 3699–3709 (1998)

Xie, Y., Chin, C.Y., Phelps, D.S.C., Lee, C.H., Lee, K.B., Mun, S., Wang, N.H.L.: A five-zone simulated moving bed for the isolation of six sugars from biomass hydrolyzate. Ind. Eng. Chem. Res. **44**(26), 9904–9920 (2005)

Xie, Y., Mun, S., Kim, J., Wang, N.H.L.: Standing wave design and experimental validation of a tandem simulated moving bed process for insulin purification. Biotechnol. Prog. **18**(6), 1332–1344 (2002)

Zang, Y., Wankat, P.C.: Three-zone SMB with partial feed and selective withdrawal. Ind. Eng. Chem. Res. **41**(21), 5283–5289 (2002)

Zhang, Z., Mazzotti, M., Morbidelli, M.: PowerFeed operation of simulated moving bed units: changing flow-rates during the switching interval. J. Chromatogr. **A1006**(1–2), 87–99 (2003)